Frascati Physics Series Vol. XXX (1997), pp. 000-000
Conference Title - Conference Town, Oct 3rd, 1996

SPECTROSCOPY OF ORBITALLY EXCITED B MESONS

Steven Goldfarb
University of Michigan, CERN-EP, 1211-Genève 23, Suisse
(on behalf of the L3 Collaboration)

ABSTRACT

We measure the mass, decay width and relative production rate of orbitally excited B mesons in Z decays registered by the L3 detector in 1994 and 1995. B-meson candidates are inclusively reconstructed and combined with charged pions produced at the primary vertex. A fit to the Bπ mass spectrum yields the masses and decay widths of the B_2^* and B_1^* spin states and the branching fraction of the mixture of all $l = 1$ spin states.

1 Event Selection

The data were collected by the L3 detector [1] in 1994 and 1995, corresponding to an integrated luminosity of 90 pb^{-1} with LEP operating at the Z mass. A total of $1,248,350$ hadronic Z decays are selected by making use of their characteristic energy distributions and high multiplicity [2]. Cutting on a $Z \to b\bar{b}$ event discriminant based on the lifetime information of charged constituents [3] yields a b-enriched sample of $176,980$ events. From a Monte Carlo sample of 6 million hadronic Z decays , the purity of the $Z \to b\bar{b}$ candidates is determined to be 83%, corresponding to a selection efficiency of 65%.

A calorimetric jet is selected for analysis as a B candidate if it is one of the two most energetic jets in the event; if a secondary decay vertex has been reconstructed from tracks associated with that jet; and if the decay length of that vertex with respect to the primary event vertex is greater than three times the estimated error of the measurement. The pion candidate is the track with the largest component of momentum in the direction of the jet and must be a constituent of the primary event vertex. These selection criteria are satisfied by $48,022$ $\mathrm{B}\pi$ pairs with a b-hadron purity of 94.2%.

2 Analysis of the $\mathrm{B}\pi$ Mass Spectrum

The combined $\mathrm{B}\pi$ mass is defined as

$$M_{\mathrm{B}\pi} = \sqrt{M_{\mathrm{B}}^2 + m_\pi^2 + 2E_{\mathrm{B}}E_\pi - 2p_{\mathrm{B}}p_\pi \cos\alpha} \quad , \tag{1}$$

where M_{B} and m_π are set to 5279 MeV and 139.6 MeV, respectively, E_{B} (p_{B}) is the measured B energy (momentum) and α is the measured angle between the B-meson and the pion. The data mass spectrum is presented in Figure 1 plotted together with the expected Monte Carlo background normalized to the region $6.0 - 6.6$ GeV.

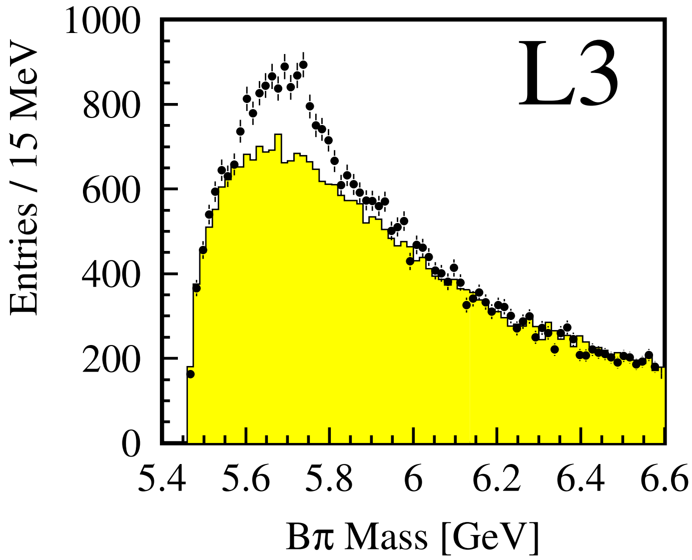

Figure 1: *Mass spectrum for selected* $\mathrm{B}\pi$ *pairs. The dots are data and the shaded histogram represents the expected background from Monte Carlo normalized to the sideband region* $6.0 - 6.6$ GeV.

2.1 Background function

The background distribution is estimated from the Monte Carlo data sample, excluding $\mathrm{B}^{**} \to \mathrm{B}^{(*)}\pi$ decays, and fit with a six-parameter threshold function given by

$$p_1(M_{\mathrm{B}\pi} - p_2)^{p_3} \exp(\mathrm{p}_4(\mathrm{M}_{\mathrm{B}\pi} - \mathrm{p}_2) + \mathrm{p}_5(\mathrm{M}_{\mathrm{B}\pi} - \mathrm{p}_2)^2 + \mathrm{p}_6(\mathrm{M}_{\mathrm{B}\pi} - \mathrm{p}_2)^3) \quad . \tag{2}$$

Parameters p_2 through p_6 are fixed to the shape of the simulated background, while the overall normalization factor p_1 is allowed to float freely. In this manner, normalization uncertainty is accounted for in the statistical error. Uncertainty due to background shape is accounted for in the systematic error by varying the shape parameters individually and studying the effect on the measurements (Sect. 2.3.1).

2.2 Signal function

2.2.1 Signal resolution

Dependence of the $\mathrm{B}\pi$ mass resolution on B^{**} mass is studied by simulating B^{**} decays at four different values of mass and Breit-Wigner width. Each signal $\mathrm{B}\pi$ mass distribution is then fit using a Voigt function: a Breit-Wigner function convoluted with a Gaussian resolution. The Breit-Wigner width is then fixed to its generated value and its mass, normalization and Gaussian resolution are extracted from the fit.

Each extracted $\mathrm{B}\pi$ mass value is found to agree with its generated mass within the statistical error of the fit and the corresponding efficiencies are found to have no mass dependence. The Gaussian resolution (Figure 2) is plotted for each mass value then fit with a linear function. This function is used in the final data fit to unfold the detector resolution at any given mass value.

2.2.2 Combined signal

According to spin-parity rules one expects to resolve mass peaks of five possible B^{**} decay modes: $\mathrm{B}_2^* \to \mathrm{B}\pi$, $\mathrm{B}_2^* \to \mathrm{B}^*\pi$, $\mathrm{B}_1 \to \mathrm{B}^*\pi$, $\mathrm{B}_1^* \to \mathrm{B}^*\pi$ and $\mathrm{B}_0^* \to \mathrm{B}\pi$. No attempt is made to tag subsequent $\mathrm{B}^* \to \mathrm{B}\gamma$ decays, as the efficiency for selecting the soft photon is low. As a result, the effective $\mathrm{B}\pi$ masses for the three decays to B^* mesons are shifted down by the $M_{\mathrm{B}^*} - M_{\mathrm{B}} = 46$ MeV mass difference. The five peaks are fit with five Voigt functions, with the relative production fractions determined by spin counting rules. Gaussian convolution to the decay widths is taken from the resolution function at each measured mass value.

Additional physical constraints, presented in Table 1, are based on predictions common to existing HQET models [4–10].

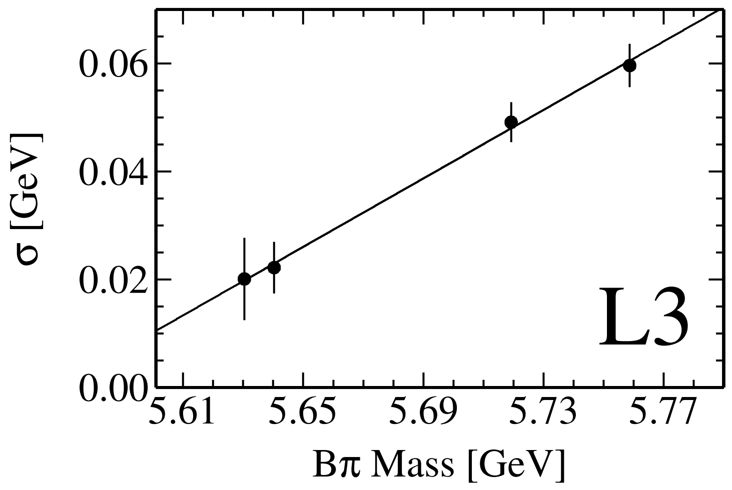

Figure 2: *Linear fit to the extracted* $\mathrm{B}\pi$ *mass resolution for Monte Carlo signal components generated at four different* B^{**} *mass values.*

j_q	Spin State	Production	Mass	Width
1/2	B_0^*	1/12	$M_{\mathrm{B}_1^*} - 12$ MeV	$\Gamma_{\mathrm{B}_1^*}$
1/2	B_1^*	3/12	free	free
3/2	B_1	3/12	$M_{\mathrm{B}_2^*} - 12$ MeV	$\Gamma_{\mathrm{B}_2^*}$
3/2	B_2^*	5/12	free	free

Table 1: *Constraints applied to the relative production rates, masses and widths of the four* B^{**} *spin states in the* $\mathrm{B}\pi$ *mass spectrum fit.*

2.2.3 Inclusion of high-mass state in fit to data

Several HQET models [5,7,10] predict the existence of radially excited ($2S$) B-meson states in the region $5.9 - 6.0$ GeV. In addition, an inclusive measurement of $\mathrm{B}\pi\pi$ final states in Z decays [11] provides evidence for a resonance in the same mass region. To account for the possible existence of these states in the mass spectrum, we fit the data including a Gaussian function in that region.

2.3 Fit results

The resulting fit, shown in Figure 3, has a χ^2 of 63 for 67 degrees of freedom. A total of 2784 events occupy the signal, corresponding to the branching fraction $\mathrm{Br}(b \to \mathrm{B}_{\mathrm{u,d}}^{**} \to \mathrm{B}^{(*)}\pi) = 0.32 \pm 0.03(stat)$, where $\mathrm{B}_{\mathrm{u,d}}^{**}$ denotes any $l = 1$ B meson containing a u or d quark. The masses and widths of the B_2^* and B_1^* mesons are found to be $M_{\mathrm{B}_2^*} = (5768 \pm 5(stat))$ MeV, $\Gamma_{\mathrm{B}_2^*} = (24 \pm 19(stat))$ MeV, $M_{\mathrm{B}_1^*} = (5670 \pm$

10(*stat*)) MeV, $\Gamma_{\mathrm{B}_1^*} = (70 \pm 21(stat))$ MeV. A total of 297 events occupy the high-mass Gaussian, denoted B′, corresponding to the branching fraction $\mathrm{Br}(b \to \mathrm{B}' \to \mathrm{B}\pi) = 0.034 \pm 0.011$. The average mass and Gaussian width of the mixture of high-mass states are found to be $M_{\mathrm{B}'} = (5.936 \pm 0.022)$ GeV and $\sigma_{\mathrm{B}'} = (0.050 \pm 0.023)$ GeV.

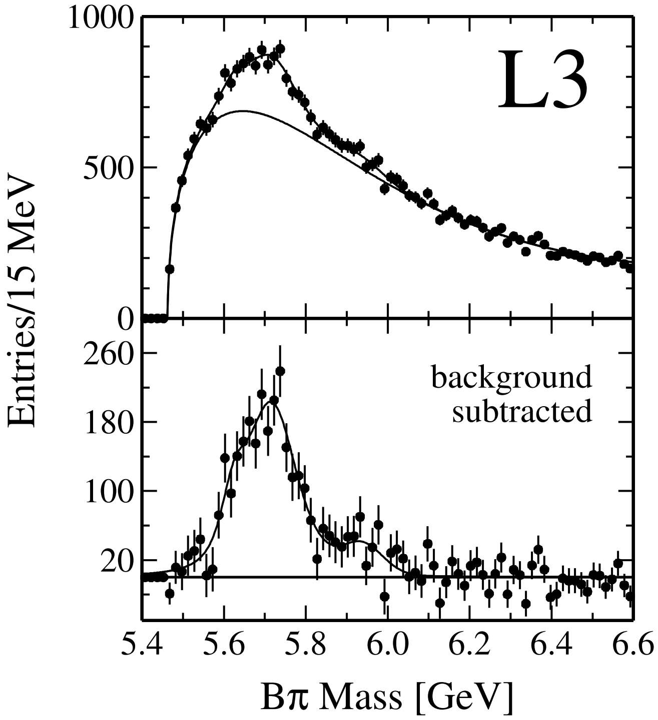

Figure 3: *Fit to the data* $\mathrm{B}\pi$ *mass distribution with the five-peak* B^{**} *signal function, Gaussian* B′ *signal function and the background function described in the text.*

2.3.1 Systematic uncertainty

Sources of systematic uncertainty and their estimated contributions to the errors of the measured values are summarized in Table 2. The b-hadron purity is varied from 92% to 96%, within the statistical error of the Monte Carlo sample. This variation affects only the overall B^{**} and B′ production branching fractions. Contribution to these errors due to uncertainty in R_b is negligible.

Systematic effects due to background modelling are studied by varying the shape parameters of the background function (parameters p_2 through p_6) and by performing the fit with other background functions. Effects due to signal modelling are studied by varying the constraints on the masses, widths, and relative production rates. The mass differences $M_{\mathrm{B}_2^*} - M_{\mathrm{B}_1}$ and $M_{\mathrm{B}_1^*} - M_{\mathrm{B}_0^*}$ are each varied within the range $5 - 20$ MeV, according to theoretical predictions. The ratios of the Breit-

Sources	$\delta M_{B_2^*}$	$\delta\Gamma_{B_2^*}$	$\delta M_{B_1^*}$	$\delta\Gamma_{B_1^*}$	$\delta Br(B_{u,d}^{**})$	$\delta M_{B'}$	$\delta\sigma_{B'}$	$\delta Br(B')$
b purity	—	—	—	—	± 0.01	—	—	± 0.007
background	± 2	± 12	± 3	± 19	± 0.06	± 2	± 2	± 0.002
mass constr.	± 4	± 7	± 4	± 7	< 0.01	± 1	± 1	< 0.001
width constr.	< 1	± 2	< 1	± 2	< 0.01	< 1	± 2	< 0.001
$B_2^* \to B, B^*$	± 2	± 4	± 1	± 2	< 0.01	± 3	± 4	± 0.003
signal resol.	± 2	± 9	± 1	± 9	± 0.01	< 1	< 1	< 0.001
signal effic.	< 1	± 1	< 1	± 1	± 0.01	< 1	< 1	± 0.001
inclusion of B'	± 3	± 17	± 12	± 12	± 0.01	—	—	—
Total	± 6	± 24	± 13	± 25	± 0.06	± 4	± 5	± 0.008

Table 2: *Sources of systematic uncertainty and their estimated contributions to the errors of the measured values. Effects due to correlations between the quantities are taking into consideration in the total error.*

Wigner widths $\Gamma_{B_1}/\Gamma_{B_2^*}$ and $\Gamma_{B_0^*}/\Gamma_{B_1^*}$ are each varied between 0.8 and 1.0. This is to account for the possibility of a slight mass dependence due to available phase space and the probability for $B^{**} \to B^{(*)}\rho$ decays [12]. Finally, the fraction of B_2^* mesons decaying to B^* mesons is varied between 1/3 and 2/3.

Effects due to uncertainty in the resolution function are estimated by varying the slope and offset of the linear parametrization. Effects due to mass-dependent variations in the signal efficiency are estimated by performing a linear parametrization of the Monte Carlo efficiencies, similar to that of the resolution, and then varying the corresponding slope and offset.

$B\pi$ pairs from the decay $B^{**} \to B\pi\pi$, for which only one of the pions is tagged, are studied as a possible source of resonant background. The resulting reflection is found to contribute insignificantly to the background in regions of small Q-value. Similarly, $B_s^{**} \to BK$ decays, for which the K is misidentified as a π, are found to contribute only slightly to the low Q-value region and their effects are included in the background modelling uncertainty contribution.

3 Conclusion

Inclusively reconstructed B mesons in $Z \to b\bar{b}$ events are combined with charged pions originating from the primary event vertex. A fit is performed to the $B\pi$ mass spectrum in the framework of Heavy Quark Symmetry and under physical constraints common to several theoretical models. The results of the fit, which provide the first measurements of the masses and decay widths of the B_2^* ($j_q = 3/2$)

and B_1^* ($j_q = 1/2$) mesons and evidence for the existence of a high-mass spin state or mix of states (denoted B') are

$$\begin{aligned}
M_{B_2^*} &= (5768 \pm 5(stat) \pm 6(syst))\ \mathrm{MeV} \\
\Gamma_{B_2^*} &= (24 \pm 19(stat) \pm 24(syst))\ \mathrm{MeV} \\
M_{B_1^*} &= (5670 \pm 10(stat) \pm 13(syst))\ \mathrm{MeV} \\
\Gamma_{B_1^*} &= (70 \pm 21(stat) \pm 25(syst))\ \mathrm{MeV} \\
\mathrm{Br}(b \to B_{u,d}^{**} \to B^{(*)}\pi) &= 0.32 \pm 0.03(stat) \pm 0.06(syst) \\
M_{B'} &= (5937 \pm 21(stat) \pm 4(syst))\ \mathrm{MeV} \\
\sigma_{B'} &= (50 \pm 22(stat) \pm 5(syst))\ \mathrm{MeV} \\
\mathrm{Br}(b \to B' \to B^{(*)}\pi) &= 0.034 \pm 0.011(stat) \pm 0.008(syst) \quad ,
\end{aligned}$$

where $B_{u,d}^{**}$ denotes a mixture of all $l = 1$ spin states and isospin symmetry is employed to account for decays to neutral pions.

These results disfavor recent theoretical models proposing spin-orbit inversion [9, 10], but agree well with earlier models [5, 7] and provide strong support for Heavy Quark Effective Theory.

4 Acknowledgements

I wish to thank Franco Fabbri for inviting me to present these results at WHS99. I also thank Chris Quigg and Adam Falk for several informative discussions on B^{**} production and decays and Maurice Gailloud for his invaluable help and guidance in the preparation of this analysis.

References

1. L3 Collaboration, Nucl. Instr. and Meth. **A 289** (1990) 35; Physics Reports **236** (1993) 1.

2. L3 Collaboration, Phys. Lett. **B 307** (1993) 237.

3. J. Branson *et al.*, L3 Note 2108, June 24, (1997). This is an L3 note freely available on request from: L3 Secretariat, CERN-PPE, 1211 Genève 23, Suisse.

4. S. Godfrey and R. Kokoski, Phys. Rev. **D 43** (1991) 1679.

5. M. Gronau and J.L. Rosner, Phys. Rev. **D 49** (1994) 254.

6. E.J. Eichten, C.T. Hill and C. Quigg, Phys. Rev. Lett. **71** (1993) 4116; Fermilab-Conf-94/118-T (1994).

7. S.N. Gupta and J.M. Johnson, Phys. Rev. **D 51** (1995) 168.

8. A.F. Falk and T. Mehen, Phys. Rev. **D 53** (1996) 231.

9. N. Isgur, Phys. Rev. **D 57** (1998) 4041.

10. D. Ebert, V.O. Galkin and R.N. Faustov, Phys. Rev. **D 57** (1998) 5663.

11. M. Feindt and O. Podobrin, DELPHI Collaboration, Submitted to the ICHEP Conference, Warsaw, July 1996, ICHEP96 Ref pa01-021.

12. Private Communication with C. Quigg, July, 1998. In addition to effects of phase space in the HQET predictions, an effective increase of the decay width may occur if the Q value is large enough to include the tail of the decay $\mathrm{B}^{**} \to \mathrm{B}\rho$. Both of these effects would cause higher-mass states to have larger decay widths.